ESRF	**Experiment title:** Tissular to subcellular imaging of Hg in rice grains	**Experiment number**: EV 240
Beamline: ID16A	**Date of experiment**: 6-7 March 2017 and 9-10 March 2017	**Date of report**: 23/03/2017
Shifts: 12	**Local contact(s)**: Murielle Salome	*Received at ESRF:*

Names and affiliations of applicants (* indicates experimentalists):

Alain Manceau

Alexandre Simionovici

ISTerre, Univ. Grenoble Alpes, CS 40700, 38058 Grenoble, France

Report:

The objective of the project was to image the intracellular distribution of Hg and other elements in natural rice grains. The Hg concentration measured on a set of grains averaged 5 ppm in the bran, 1 ppm in the germ, and 0.5 ppm in the endosperm. The review committee considered that it was "*An excellent proposal, although the panel is concerned about the possibility to detect such low concentrations*".

Another difficulty, which we had not anticipated, was the sample preparation. Cryo-microsectioning of several rice grains (not embedded and embedded in OCT) was attempted by Hiram Castillo at the ESRF but was not successful due to the brittle nature of the endoderm which resulted in pulverization of the sliced sections. After several trials, and much determination and perseverance, cryomicrotomic sections of 5 microns thickness from the softer germ were obtained. However, the sections would not stick to the Si_3N_4 windows in liquid nitrogen. Therefore, it was decided to warm up the sections to have them adhere on windows. Examination under optical microscope (Fig. 1) showed that the germ tissue and cell integrity were reasonably well preserved. In the end, two sections were mounted on the cryo-holder of the beamline and mapped. Low temperature measurements are necessary to not vaporize Hg under the beam.

In parallel to the microsectioning attempts at the ESRF, ultramicrotome sectioning was attempted by Karine Rousseau (SERMA Technologies) and François Saint-Antonin (Plateforme CEA MET OSIRIS), care of Murielle Salome. The sections themselves looked good, except that sectioning produced debris which would have detached from the window contaminating the beamline KBs if they had been mounted in the cryo-holder (Fig. 2). These sections were disregarded.

Several nano-XRF maps were recorded at 200 nm, 70 nm and 50 nm steps, and at 200 ms to 250 ms counting time. The preparations were stable under the nanofocused beam and the Hg(Lα) line detected, as shown by the XRF spectral fits with/without the Hg lines (Fig. 3). Therefore, sample concentration does not appear to be an issue. However, the Hg(Lα) line sits on the tail of the intense Au(Lα) parasitic line from the cryo-holder and was barely visible. As a consequence, the Hg(Lα)

map is a shadow image of the Au(Lα) map produced by the fluorescence of the cryo-holder induced by the scattered beam at the excitation energy of 17 keV (Figs. 4 and 5). This spurious effect was observed on all maps preventing Hg from being imaged. Quantification requires no Au contamination. Mercury imaging was further hampered by the fact that six detectors were on repair out of nominally twelve, thereby decreasing the total counting rate (i.e., statistics) by two.

A cure for the overlapping Au/Hg fluorescence lines would be to weld a plate of thickness ≥ 0.5 mm on top of the Au cryo-holder made of a metal of high thermal conductivity which has no lines contaminating the Hg(Lα) line at 9.98 keV and the Hg(Lβ) line at 11.9 keV. Care should be also exercised to not saturate the detectors with a high deadtime for it would prevent measuring efficiently the Hg(Lα) counts. A silver plate would be suitable. Thermal conductivity *k* (W/m·K) is 315 for Au and 407 for Ag, therefore the cryogenics would work. Spectroscopically, the Ag L lines are at 2.9-3.1 keV, thus much less excited by the incident 17.0 keV X-rays, and they would not interfere with Hg L lines.

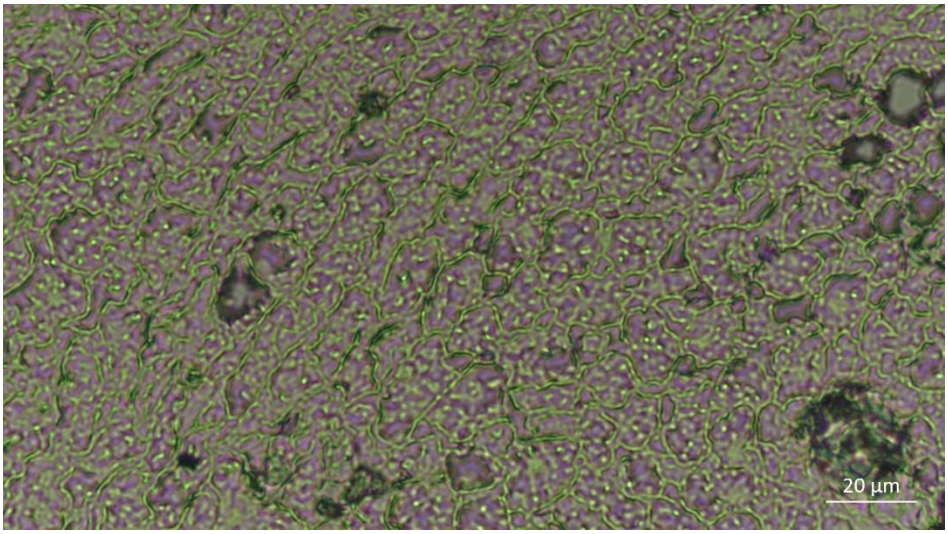

Fig. 1. Optical micrograph of a cryomicrotomic section from a germ.

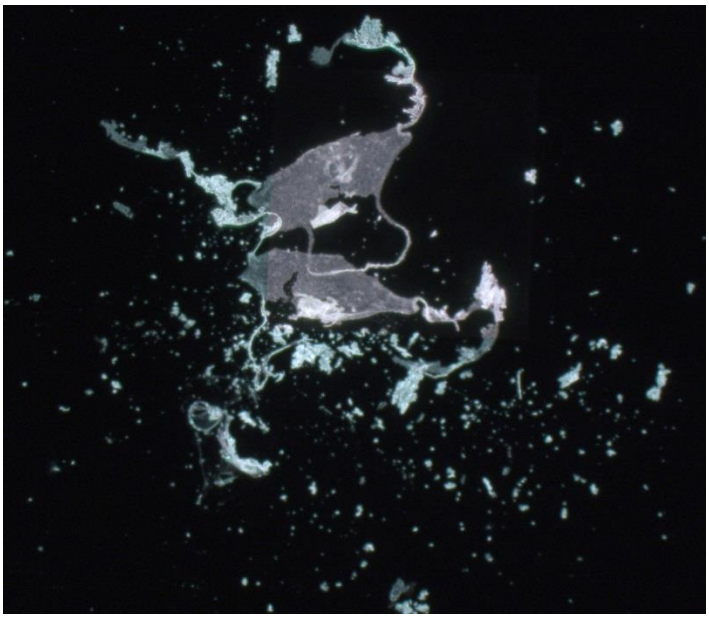

Fig. 2. Optical micrograph of a cryo-ultramicrotomic section of a germ littered with debris.

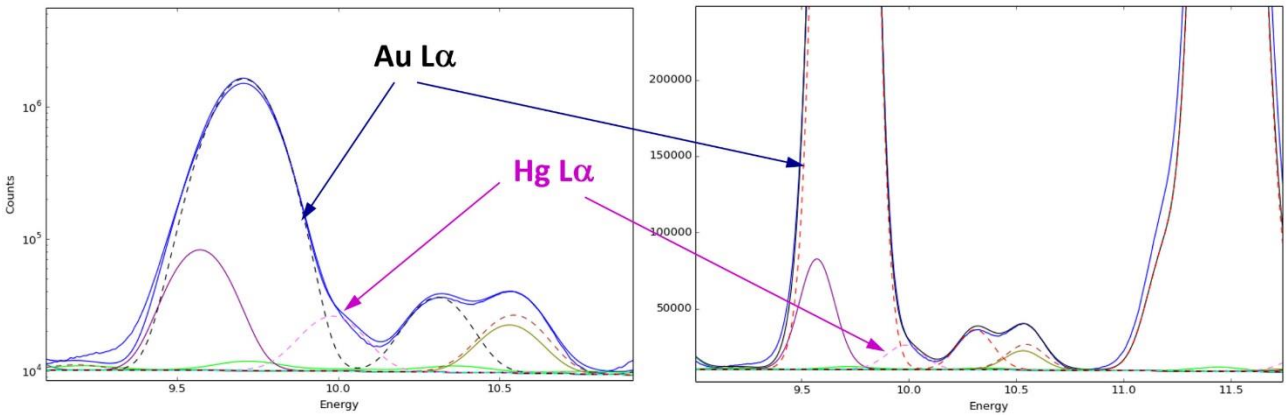

Fig. 3a. Blue line: Sum of the nano-XRF data over all pixels from the region mapped in Figure 4. Color lines : Decomposition of X-ray emission lines used to image K, Au and Hg in Figure 4. Left: log scale. Right: linear scale.

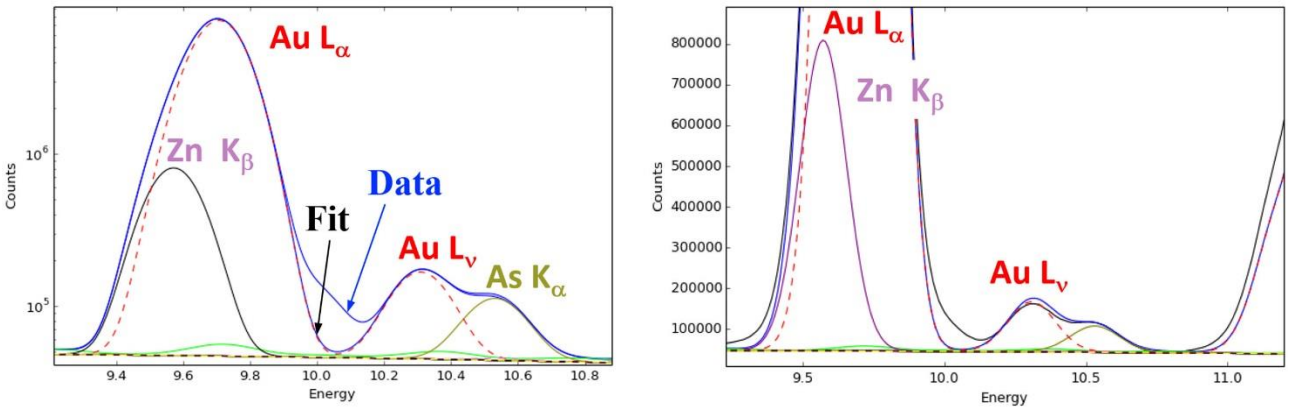

Fig. 3b. Same as Fig. 3a, but with Hg omitted in the decomposition.

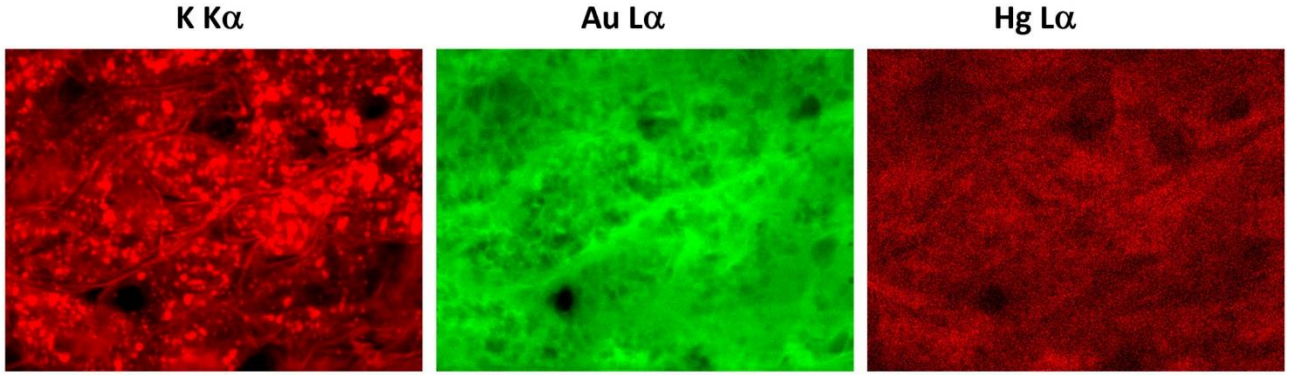

Fig. 4. Nano-XRF elemental maps of the germ tissue collected at 50 nm steps showing good cellular preservation with clearly visible cell walls and internal ultrastructures.

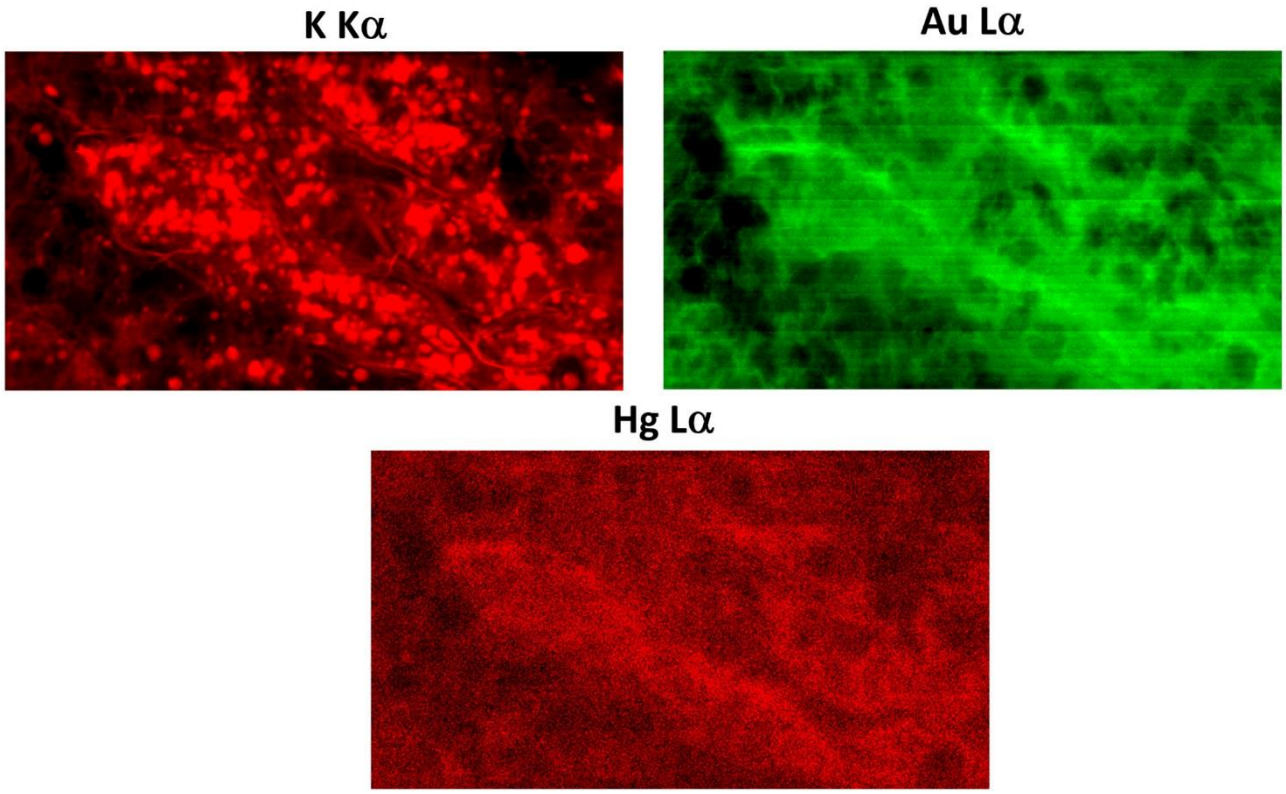

Fig. 5. Nano-XRF elemental maps from another region of the germ tissue collected also at 50 nm steps and showing again good cellular preservation with clearly visible cell walls and internal ultrastructures.